ACS APPLIED MATERIALS & INTERFACES

Albright COLLEGE

Subscriber access provided by ALBRIGHT COLLEGE

Surfaces, Interfaces, and Applications

Ultra Low Temperature Cofired Ceramic Substrates with Low Residual Carbon for the Next Generation Microwave Applications

Nina Joseph, Jobin Varghese, Merja Teirikangas, Timo Vahera, and Heli Jantunen

ACS Appl. Mater. Interfaces, **Just Accepted Manuscript** • DOI: 10.1021/acsami.9b07272 • Publication Date (Web): 11 Jun 2019

Just Accepted

is published by the American Chemical Society. 1155 Sixteenth Street N.W., Washington, DC 20036

Ultra Low Temperature Cofired Ceramic Substrates with Low Residual Carbon for the Next Generation Microwave Applications

Nina Joseph*, Jobin Varghese, Merja Teirikangas,
Timo Vahera, and Heli Jantunen

Microelectronics Research Unit, Faculty of Information Technology and Electrical Engineering, University of Oulu, Finland, P.O. Box 4500, FI-90014.

*Corresponding author: Nina Joseph

Email: ninajoseph11@gmail.com

Abstract

High temperature cofired ceramics (HTCCs) and low temperature cofired ceramics (LTCCs) are important technologies in the fabrication of multilayer ceramic substrates for discrete devices, electronics packages and telecommunications. However, there is a place and need for materials with lower fabrication temperatures to decrease the associated energy consumption. The present paper studies the feasibility of two ultra-low sintering temperature cofired ceramic (ULTCC) materials, copper molybdate and copper molybdate-Ag_2O, sinterable at 650 and 500 °C respectively, for multilayer substrates using tape casting. The slurry composition developed uses environmentally friendly organics and non-toxic binder and solvent. Additionally, the green cast tapes exhibit very low residual carbon (less than 5%) after sintering on analysis by X-ray photoelectron spectroscopy. The multilayer substrates show permittivity values of about 8 with a low dielectric loss in the range of 10^{-5} to 10^{-4} in the frequency range of 2-10 GHz along with a low coefficient of thermal expansion in the range of 4-5 ppm/°C and good compatibility with an Al electrode. Thus, these proposed substrates have much promise, with good thermal, mechanical and dielectric properties comparable to commercial substrates while also providing an energy and environment-friendly solution.

Keywords: $CuMoO_4$; ULTCC; Environmental friendly; Tape casting; Microwave substrates

Introduction

Ultra-low temperature cofired ceramic (ULTCC) technology has attracted interest recently due to its efficient energy saving as compared to the conventional High Temperature Cofired Ceramic (HTCC) and Low Temperature Cofired Ceramic(LTCC) technologies.[1] LTCC has been the standard technology for the integration of components and substrates for high-frequency applications for several decades. LTCC technology enables the tape casting of dielectric materials for multilayer structures cofired with metal electrodes at a low temperature (~ 850 °C). For microwave applications

the used dielectric materials must have a low dielectric constant to increase the signal speed, a low dielectric loss to improve the frequency selectivity and the substrates are expected to meet the requirements imposed by growths in technology. Compared to the printed circuit board (PCB) materials, the ceramics can provide better thermal stability with a low thermal expansion coefficient and high thermal conductivity as well as a high integration potential to deliver good performance at high frequencies.[2,3] In the case of ULTCC technology the sintering temperature is commonly much less than 700 °C, thus enabling lower energy consumption and easier integration of different materials into the same multilayer structure[4] while at the same time being feasible for the same application areas as LTCC technology.[1] This technology provides an alternate path to solve the problem of energy crisis by conserving the existing energy used in the present technology rather than looking for new source of energy and is a simple, easy and cheap method.

In the last five years several ULTCC compositions have been reported,[1,4-8] but only a few of them have been explored for multilayer substrates through tape casting with a low burn out temperature[9-13] and our work is an attempt to examine this aspect. In this work**,** the focus is on the investigation of the environmentally friendly processing aspects of tape casting formulations which are based on the non-toxic chemical solvent dimethyl carbonate[14,15] together with a biodegradable and biocompatible binder of poly(propylene carbonate).[10] This binder system has been successfully used for tape casting of ULTCC compositions[10,12,13] which have a lower burnout temperature. However, no studies on the carbon content of the cast tape before and after sintering have been reported. The carbon analysis gives information about the carbon emission during the processing as well as the residual carbon of the substrate. This is an important aspect of this work since residual carbon can degrade the dielectric properties of the final product.

In our previous research, it was observed that $CuMoO_4$ ceramic exhibits good thermal and dielectric properties with an excellent densification of 96% by sintering at 650 °C and its composite obtained by adding 0.5 wt.% of Ag_2O was also a good candidate for substrate applications with a much lower sintering temperature of 500 °C. These studied ceramics also exhibited good chemical compatibility with aluminium, which can be used for embedded electrodes.[16, 17] Hence, our present work is an attempt to transform these ULTCC materials into ULTCC substrates by tape casting using an environmentally benign slurry composition and post processing techniques such as multilayer lamination, screen-printing and co-firing, together with an investigation of their microstructural, dielectric and thermal characteristics.

Materials and Methods

Preparation of $CuMoO_4$ ceramic and $CuMoO_4$ –Ag_2O ceramic composite

The $CuMoO_4$ ceramic (CMO) was prepared using the solid-state ceramic route by mixing stoichiometric amounts of high purity CuO (> 99%, Alfa Aesar) and MoO_3 (> 99%, Alfa Aesar) in ethanol medium for 12 h, with subsequent drying followed by calcination at 550 °C. $CuMoO_4$–Ag_2O ceramic composite (CMOA) was prepared by mixing 0.5 wt.% of Ag_2O (99+%, Alfa Aesar) into the CMO powder in the ethanol medium for 12 h, followed by drying.

Preparation of CMO and CMOA substrates by tape casting

To prepare the tape casting slurry, dimethyl carbonate (DMC) (Sigma Aldrich, St. Louis, MO) was used as the solvent with poly(propylene carbonate) (PPC) (QPAC40, Empower Materials, New Castle, DE) as the binder and butyl benzyl phthalate (S160, Richard E. Mistler, Yardley, Pennsylvania) and polyethylene glycol (UCON 50HB2000, Richard E. Mistler) as the type I and type II plasticizers respectively. Initially, the ceramic powder (CMO/CMOA) was mixed with dimethyl carbonate and poly(propylene carbonate) for 12 h by ball milling. The milling was continued for 24 h after the addition of the two plasticizers. The resultant slurry was cast on a silicone-coated Mylar carrier tape at a speed of 0.8 m/min using a laboratory caster (Unicaster 2000, Leeds, UK) and a 400 μm doctor blade. The dried green cast tape was peeled off for further processing. Aluminium ink (AL-PS1000, Applied Nanotech, Inc., USA) co-firable in the temperature range of 500-650 °C was screen printed followed by drying at room temperature for co-firing analysis, which is performed in the normal air atmosphere. For further characterization, five green cast tapes were stacked by vacuum lamination and isostatic pressing at 75 °C, 20 MPa for 10 min (Turbovac 430 STE vacuum machine and PTC IL-4008, Isostatic laminator). The stacked tapes were sintered at their respective sintering temperatures (CMO-650 °C /2h; CMOA-500 °C /2h) with an optimized sintering profile. The process flowchart is shown in figure 1.

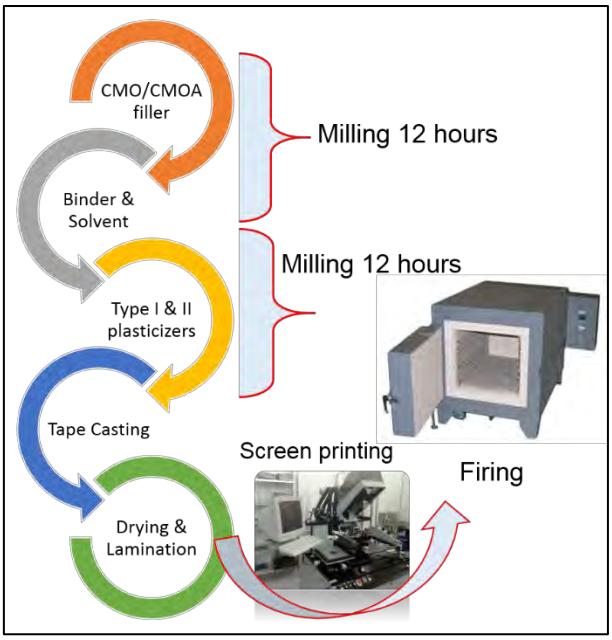

Figure 1: *Tape casting and post processing flow chart*

Two commercial LTCC tapes 9k7 (single green layer thickness 0.249 mm) and 951 (single green layer thickness 0.251 mm) (Dupont, US) were used to compare the XPS measurement results. The four-layer stacks were sintered at 850 °C and had thicknesses of 0.822 and 0.864 mm, respectively.

Characterization

The particle size and specific surface area of the ceramic powders were analysed using the laser diffraction method (Beckman Coulter LS13320) and a particle surface area analyzer (G.W. Berg & Co. Micrometrics ASAP 2020), respectively. Tensile strength of the green cast tapes was measured by a tensile strength measurement setup (TST 350, Linkam Scientific Instruments Ltd., Survey, UK) and Linksys 32 software at room temperature with a speed of 100 µm/s using standard dumb-bell shaped samples (length 36.2 mm and width of 3.1 mm). The burnout of the organic additives was studied using differential scanning calorimetric (DSC) measurement/thermogravimetric analysis (Netzsch 404 F3, Selb). The bulk density of the sintered samples was measured in an ethanol medium using the Archimedes method. The shrinkage was calculated from the dimensions of the laminated and sintered substrates. For XPS analysis, a Fisher Scientific, ESCALAB 250 Xi using the MgKα X-ray source was used and the spectrometer was calibrated with reference energies of Au $4f_{5/2}$ (83.9±0.1 eV) and Cu $2p_{3/2}$ (932.7±0.1 eV). An angle of 90° was maintained between the surface and the analyser (take-off angle) for the measurement. The C 1s peak witha binding energy at 284.8 eV corresponding to the surface contamination was used for binding energy calibration for the sample charging correction.[18,19] The surface roughness of the green and sintered substrates was measured using an Atomic Force Microscope (AFM, Veeco dimension 3100 130 SPM) operating

in the contact mode regime and their microstructure was analyzed using field emission scanning electron microscopy (Zeiss Ultra Plus, Germany). Microwave dielectric properties of the green and sintered substrates were measured by the split-post dielectric resonator (SPDR) (QWED, Poland) technique using a vector network analyser (10 MHz to 20 GHz, Rhode & Schwarz, ZVB20, Germany) and their temperature dependence by using a furnace (Espec SU-261) operating at -40 to 80 °C integrated with the microwave measurement setup. With this method, the total uncertainty of the determination of the relative permittivity was about 0.5% and the dielectric loss was in the range of 10^{-5}.[20,21] Cylindrical samples of 8 mm × 15 mm were used to measure the linear coefficient of thermal expansion (CTE) using a dilatometer (NETZSCH DIL 402 PC/4, Germany).

Results and discussion

Tapecasting and lamination

The CMO and CMOA powders had an average particle size in the range of 2.3-2.5 µm with a surface area of ~ 3.5 m^2/g. These ceramic powders properties are in the range considered desirable to obtain an optimized slurry composition for tape casting[12] as they have a considerable influence on the green cast tapes by determining their quality, strength and flexibility.[22] The surface area determines the interaction of the ceramic with the organic additives and the moderately small particle size helps in the uniform dispersion of the fillers in the slurry. Since CMO and CMOA show a similar particle size and density, the slurry composition (Table 1) used is same for both of them.

Table 1: *Slurry composition for the tape casting*

Ingredients	Materials	Content (wt.%)
Ceramic powder	CMO/CMOA	50
Binder	PPC – poly(propylene carbonate)	3.6
Plastizicer-I	BBP -Butyl benzyl phthalate	1.2
Plastizicer-II	PEG - Polyethylene glycol	1.2
Solvent	DMC - dimethyl carbonate	44

The chemical nature of the organic ingredients used in the tape casting slurry has an effect on the surrounding environment. Although water would be environmentally the ideal solvent, it has many disadvantages in tape casting due to its slow evaporation rate and agglomeration,etc.[23] The problem was solved by using DMC, which is reported to be a highly reactive non-toxic solvent and as a dispersant.[14,15] PPC is known as an environmentally friendly binder [24-26] as it leaves a low residue after burnout and has a low burn out temperature. The green cast tapes of CMO and CMOA had a single layer thickness of 0.111 and 0.120 mm, respectively. The mechanical strength of the green tapes is important for further processing. The single layer tensile strengths of these CMO and CMOA

tapes were 0.17 and 0.19 MPa, respectively, with a standard deviation of 0.02. These values are comparable to some of the reported LTCC tapes[27,28] but are of course lower than the commercial LTCCs due to their well optimized slurry composition and harder binders that can be used at the higher sintering temperature.

Sintering and co-firing

The TG/DSC analysis of the green cast tapes shown in figure 2 gives an overall idea about the burnout temperature of the organic additives. It is necessary to annihilate the organic additives before sintering to prevent their effects on the shrinkage or electrical properties of the sintered substrates. A managed burnout also minimizes defects such as delamination, cracking and anisotropic shrinkage during sintering.[29] It was observed that the weight loss was slow for both the tapes up to 150 °C with a sharp increase to about 10% in the temperature range of 150-250 °C, corresponding to the removal of binder and plasticizer. Also, exothermic peaks could be observed around 200-230 °C in the DSC: these were due to the strong decomposition of the low molecular weight organics such as the binder and plasticizer. The TG and DSC curves of both green cast tapes were similar because the type and amount of organics used in the tapes were the same. However the small peak at around 400 °C observed in the DSC of the CMOA tape was due to the formation of a new compound, $Cu_2Ag_2(MoO_4)_3$, due to the reaction of Ag obtained by the decomposition of Ag_2O with $CuMoO_4$ and was expected to melt around 500 °C, as we have reported earlier.[17]

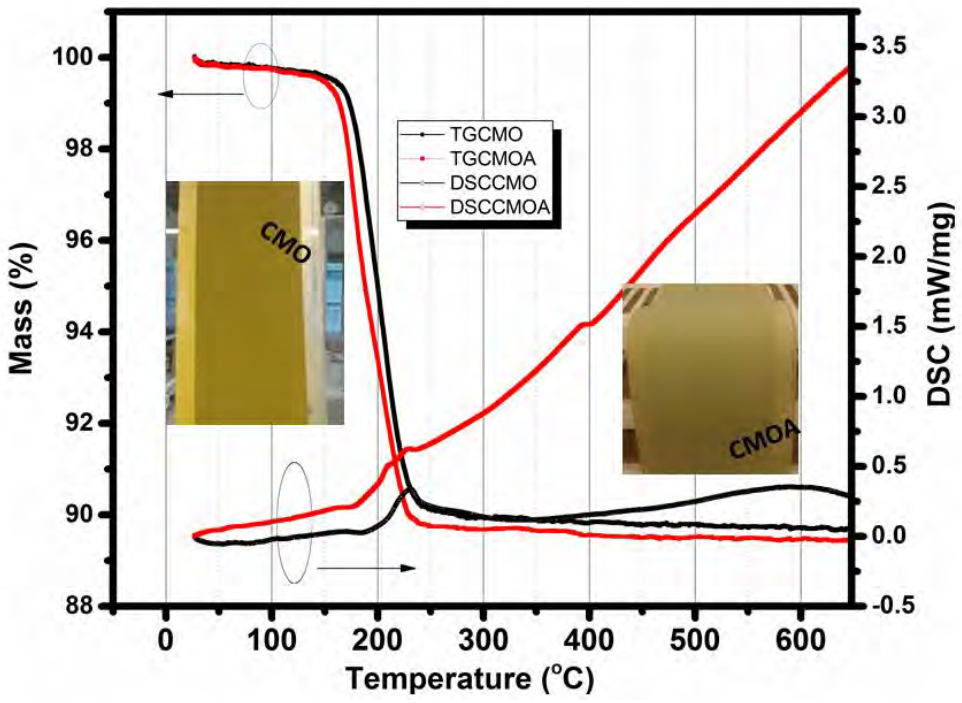

Figure 2: *TG/DSC curve of CMO and CMOA green cast tapes (Inset figure: Photographic images of the green cast tapes).*

TG analysis of the individual constituents, slurry without and slurry with the ceramic was done to gain more detailed information on the thermal decompositions (figure 3). It is clear that the solvent was removed first below 100 °C (figure 3 (a)). After that the binder removal started below 200 °C and ended at about 300 °C (figure 3 (b)), when the plasticizers were also removed (figure 3 (c & d)). The removal phase of the individual components from the slurry without the ceramics are clearly visible from figure 3 (e), where a weight loss of 50% occurred below 100 °C (solvent) and the rest was removed between 200 and 300 °C (due to binder and plasticizers). Figure 3 (f & g) gives information on the TG of the green cast tapes where a weight loss of about 10% occurred below 250 °C. The presence of ceramic is evident as it corresponds to the decrease in the decomposition temperature as compared to the individual constituents shown in figure 3. The green cast tapes used were dried and hence a low weight loss below 100 °C owing to the solvent was observed. It is also clear from the figure 3 (a, b, c, d & e) that the weight loss was almost 100% indicating a high level of burnout of the organics. However, it was difficult to achieve a complete residual-free tape after sintering due to the trapping of the organics, and the corresponding low residual carbon content is further confirmed by XPS.

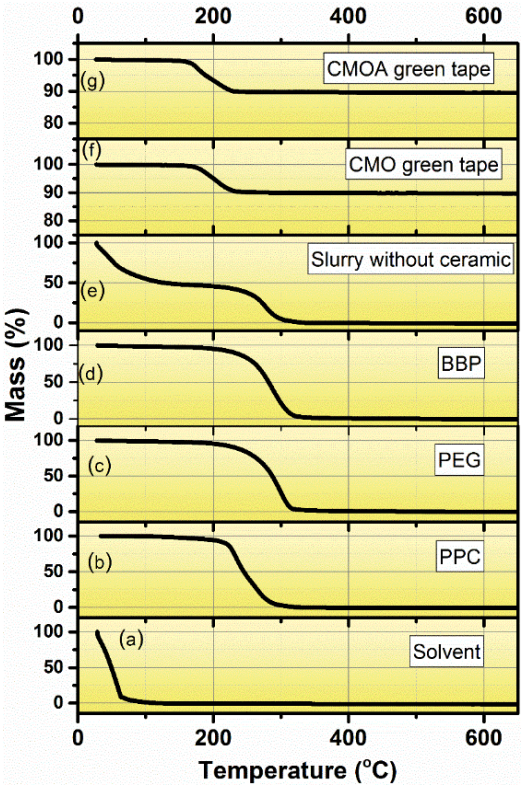

Figure 3: *TG curve of ingredients used in the present tape casting composition (a-d), slurry without ceramic (e) and green cast tapes (CMO (f) and CMOA (g)).*

Based on these results, the sintering profile of the substrates was carefully optimised by varying the sintering rates and dwell time to obtain a densified tape with uniform microstructure affecting the performance of the final module.[22,30] Figure S1 in the supporting information gives the effect of sintering rate and intermediate dwell time on the densification of the CMO substrate. A faster heating rate with a minimum intermediate dwell time increases the densification, which corresponds to the fast grain growth. Figure 4 shows the optimised sintering profile of the CMO and CMOA substrates. Both substrates had the same sintering profile with a difference only in their sintering temperature, because the type and amount of organic additives used were the same. The removal of the organic components was ensured by 1 h dwell time at 350 °C. The CMO was well sintered with 95% densification after sintering at 650 °C, and about the same value was achieved in the CMOA (96%) with a lower sintering temperature (500 °C) due to the formation of a low melting compound.[17] These densification values are almost the same as those reported earlier for the bulk samples.[16,17] Five-layer stacks of sintered CMO and CMOA substrates were produced with a thickness of 0.430 and 0.450 mm, respectively. The sintered stacks shown in the inset of figure 4 were hard and robust with a deep green color.

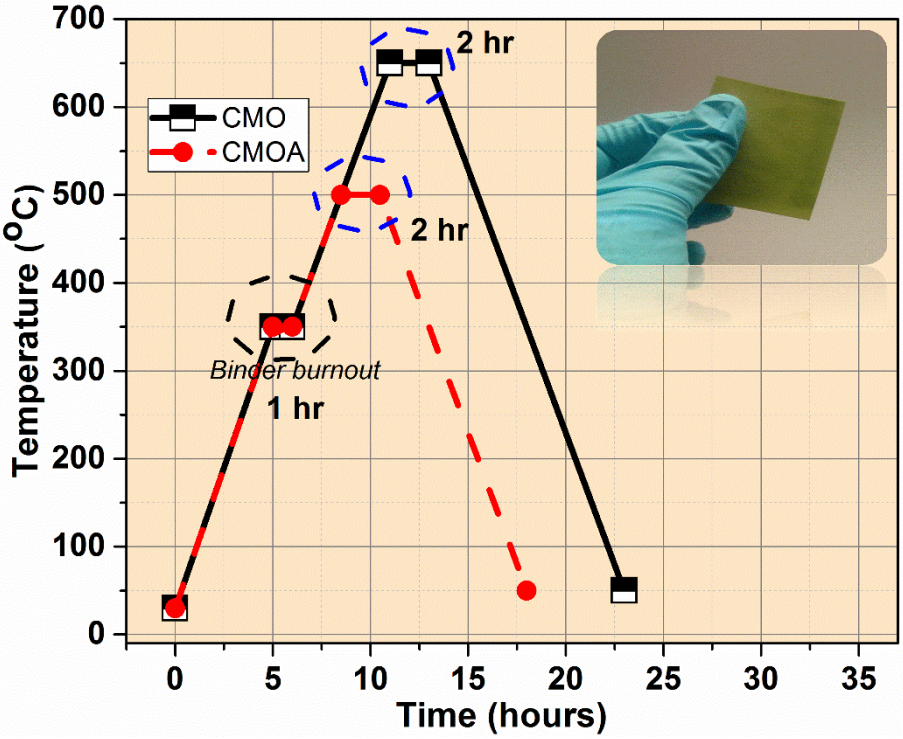

***Figure 4**: Sintering profile of CMO and CMOA substrates (Inset figure: Photographic image of the sintered substrate).*

The sintered substrates had a shrinkage of 15±1, 14± 1 and 12±2% respectively in the X, Y and Z direction for the CMO stacks, and 16.5±1, 16.0 ±1and 14± 2% respectively for the CMOA, which are in the desired range for commercial production.[31] Shrinkage is important for practical substrate applications as it restricts the substrate size that can be processed, which may create complexity in the processing as well as in the embedded passive components.[32]

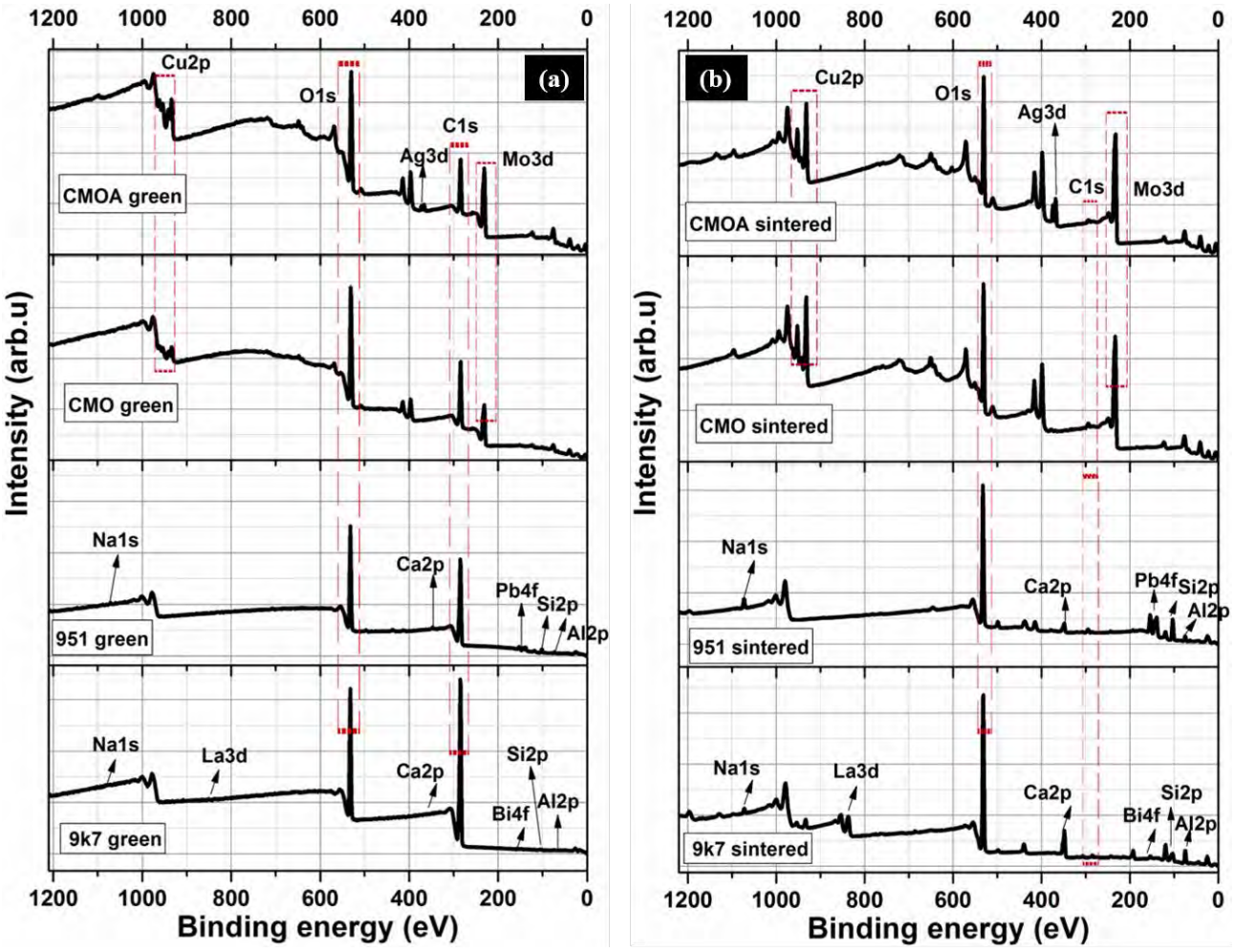

Figure 5: *XPS survey spectra of (a) green (b) sintered substrates (commercial 9k7 & 951, CMO & CMOA substrates)*

XPS surface analysis was performed on the green and sintered substrates (CMO &CMOA) to obtain more information on the residual carbon, and the results were compared with the commercial LTCC substrates 9k7 and 951.[18,19] The survey spectra of the green and sintered 9k7, 951, CMO and CMOA substrates shown in figure 5 (a) and (b) provide an insight into the carbon content of these substrates. Highly intense C1s peaks which are seen for the green substrates (figure 5 (a)) become barely visible in the spectra of the sintered samples 5 (b). High-resolution C1s spectra of the green and sintered substrates are given as figure S2 in the supplementary information. The decrease in the carbon content with sintering is more evident from Table 2, which presents the atomic wt.%. It is clear that the carbon

content was less than 5 wt.% in both the substrates after sintering and can also be accounted within the error limit owing to the surface carbon atoms due to the surface roughness of the substrate compared with the XPS analysis depth. Hence, the results are in agreement with the TG analysis depicted in figure 3. The results are well in line with the results for the commercial LTCC substrates.

Table 2: Atomic wt.% of carbon in the green and sintered commercial 9k7 & 951, CMO & CMOA substrates

Sample name	**Carbon atomic wt.%** ±1.5%	
	Green	Sintered
CMO	40.2	4.5
CMOA	44.4	4.3
951	65.2	5.1
9k7	75.8	3.0

Moreover, the carbon content in the ULTCC substrate was lower and possibly corresponds to the composition as well as the molecular weight of the organics used to obtain a lower burnout temperature. This in turn can reduce the carbon burnout, which is an added advantage of these ULTCC compositions. These results indicate that the composition used in the present work provides much less carbon burnout as well as less residual carbon, which is a both necessity and a great advantage to the future electronics and communication industry.

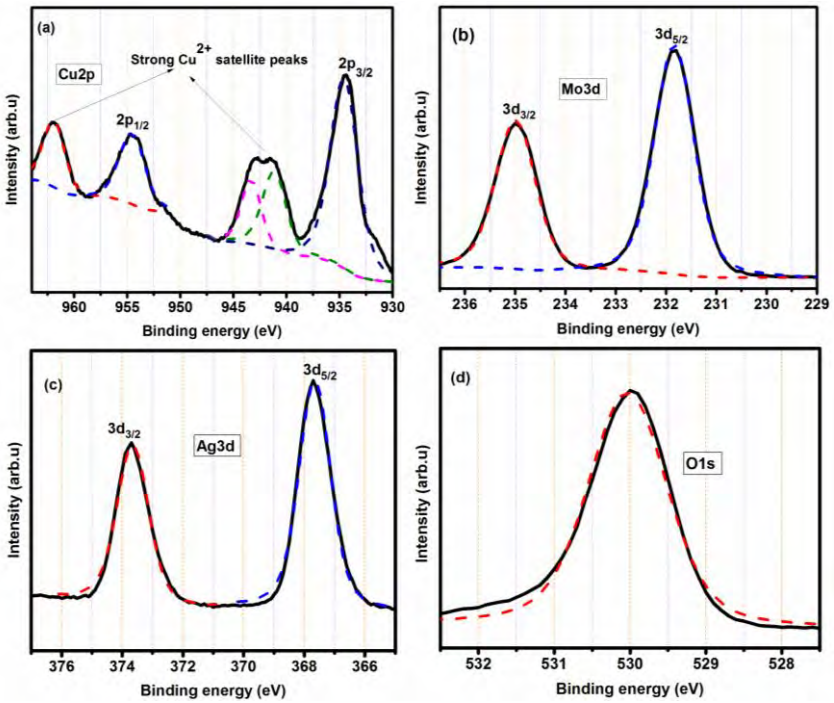

Figure 6: *High resolution spectra of (a) Cu2p (b) Mo3d (c) Ag3d (d) O1s of sintered CMOA substrate.*

Figure 6 presents the high resolution Cu2p, Mo3d, Ag3d and O1s spectra and the curve level fitting observed for sintered CMOA ceramic in which the Cu2p, Mo3d, O1s spectra are similar to those of CMO as it is the major phase.[16] The high resolution Cu2p (figure 6 (a)) shows the spin-orbital splitting

components of $2P_{3/2}$ and $2p_{1/2}$ by about 19.98 eV while the FWHM of the corresponding peaks are 3.11 and 2.86 eV respectively. Strong satellite Cu^{2+} peaks are also observed indicating the oxidation state of Cu. The high resolution spectrum of Mo 3d (figure 6 (b)) shows the spin-orbital splitting $3d_{5/2}$ and $3d_{3/2}$ having an orbital split of about 3.15 eV and FWHM of 0.92 and 0.93 eV respectively.[16,33] The high resolution Ag3d spectrum (figure 6 (c)) exhibits spin- orbital splitting $3d_{5/2}$ and $3d_{3/2}$ by about 6 eV with FWHM of 1.25 eV and 1.24 respectively. This further confirms the presence of Ag in CMO, which is difficult to observe due to its low amount. The O 1s photoelectron peak at about 530 eV depicted in figure 6 (d) gives information on the oxide ion in the sintered substrate with different chemical bonding and possibly corresponds to the bridging oxygen atoms, showing good agreement with reported values.[16,19,34] The fitted binding energies of Cu2p, Mo3d, Ag3d and O1s are given in supporting information Table S1.

Surface analysis and microstructure

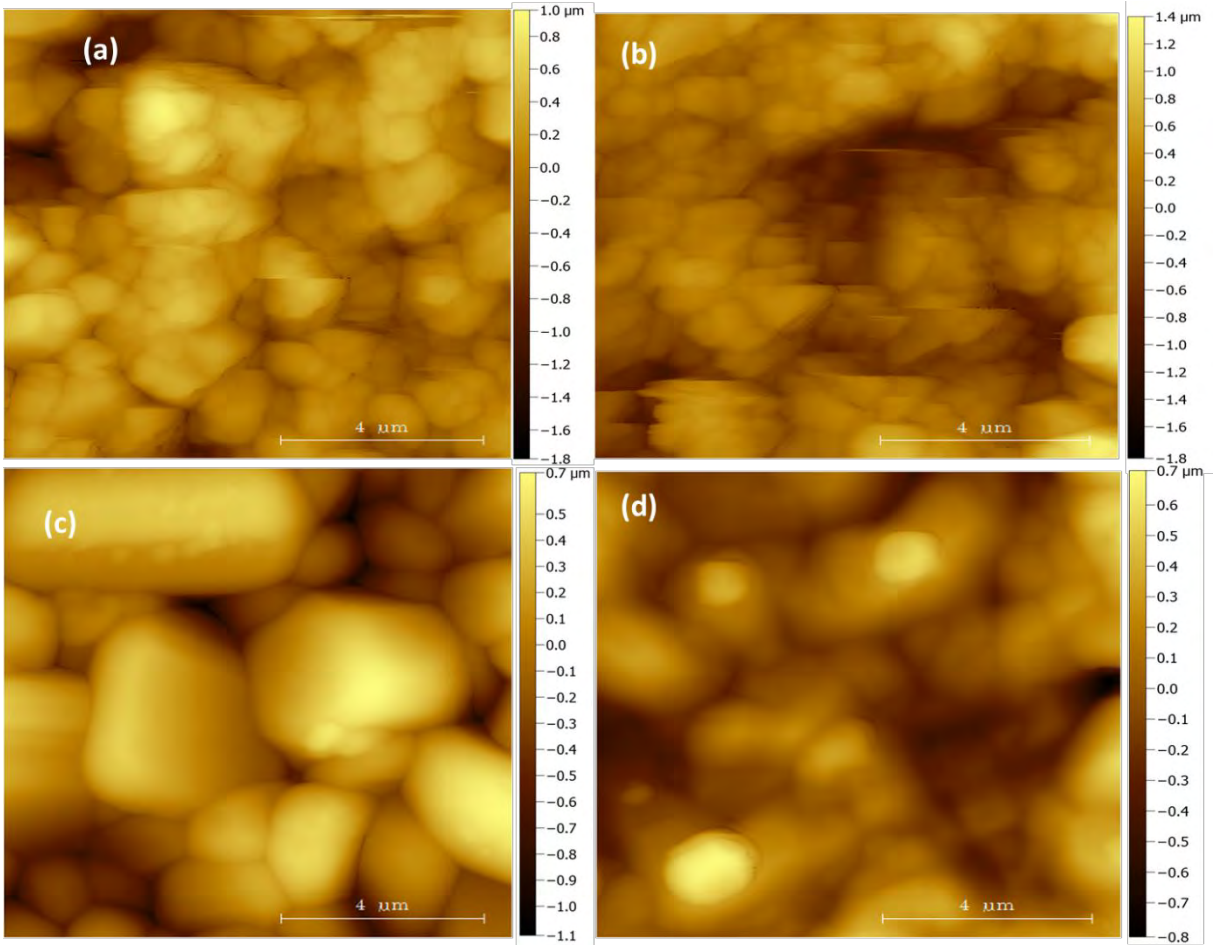

Figure7: *2D AFM images of green (a) CMO (b) CMOA and sintered (c) CMO (d) CMOA substrates*

The surface quality of the tapes and sintered substrates is critical for microelectronic applications because it influences the accuracy of the printed electrodes and their performance through the skin-depth at high frequencies. Two-dimensional (2D) AFM images of the green and sintered substrates

shown in figure 7 and the corresponding three dimensional (3D) images shown in the supporting information figure S3 indicate that the grains were distributed in the form of hills and valleys. It is also clear that the grains were larger after sintering, which indicates grain growth as well as the removal of organics. Analysis the topography scans of the sample surfaces provides the roughness parameters, which includes average roughness (Ra), root mean square roughness (RMS), skewness (Skew) and kurtosis. The roughness parameters of the tapes are given in the in Table 3. The CMO and CMOA green tapes exhibited average surface roughness of 257±11% and 302±10%, respectively, which is reported to be comparable to commercial LTCC tapes.[35,36] The skew value measures the asymmetry of the surfaces, and both the green tapes had a negative skew value of -0.6 and -0.1, which indicates that they had good bearing surfaces and were suitable for device fabrication. The negative value indicates that the surfaces had a longer tail distribution below the reference plane i.e. thevalleys were predominant on the surface of the tapes, which is also evident from the 2D and 3D images. Kurtosis measures the distribution of the spikes above and below the mean line/plane.[36,37] The green tapes had a kurtosis of 0.9-0.7, meaning that the surface was flatter and is referred to as platykurtic. The kurtosis value indicates that the surface was not spiky but bumpy which is in agreement with the images.[37,38] Similarly, for the sintered CMO and CMOA substrates, the average surface roughness decreased to 157±6% and 172±5% nm, respectively. The low average surface roughness may correspond to the uniformity of the surface obtained by sintering after the removal of all the organic additives as well as to the increased densification. The positive skew value of 0.6 (CMO) and 0.3 (CMOA) indicates the brittle nature of the sintered tapes. Similar to the green substrates, the sintered substrates also had bumpy surface rather than spikes as their kurtosis value was less than 3 (0.4 and 0.1),[35-38] which is also evident from the images.

Table 3: *Surface quality of the green and sintered substrates*

Surface parameters	**Green tape**		**Sintered tape**	
	CMO	**CMOA**	**CMO**	**CMOA**
Ra (nm)	257	302	157	172
RMS (nm)	329	380	202	215
Skew	-0.6	-0.1	0.6	0.3
Kurtosis	0.9	0.7	0.4	0.1

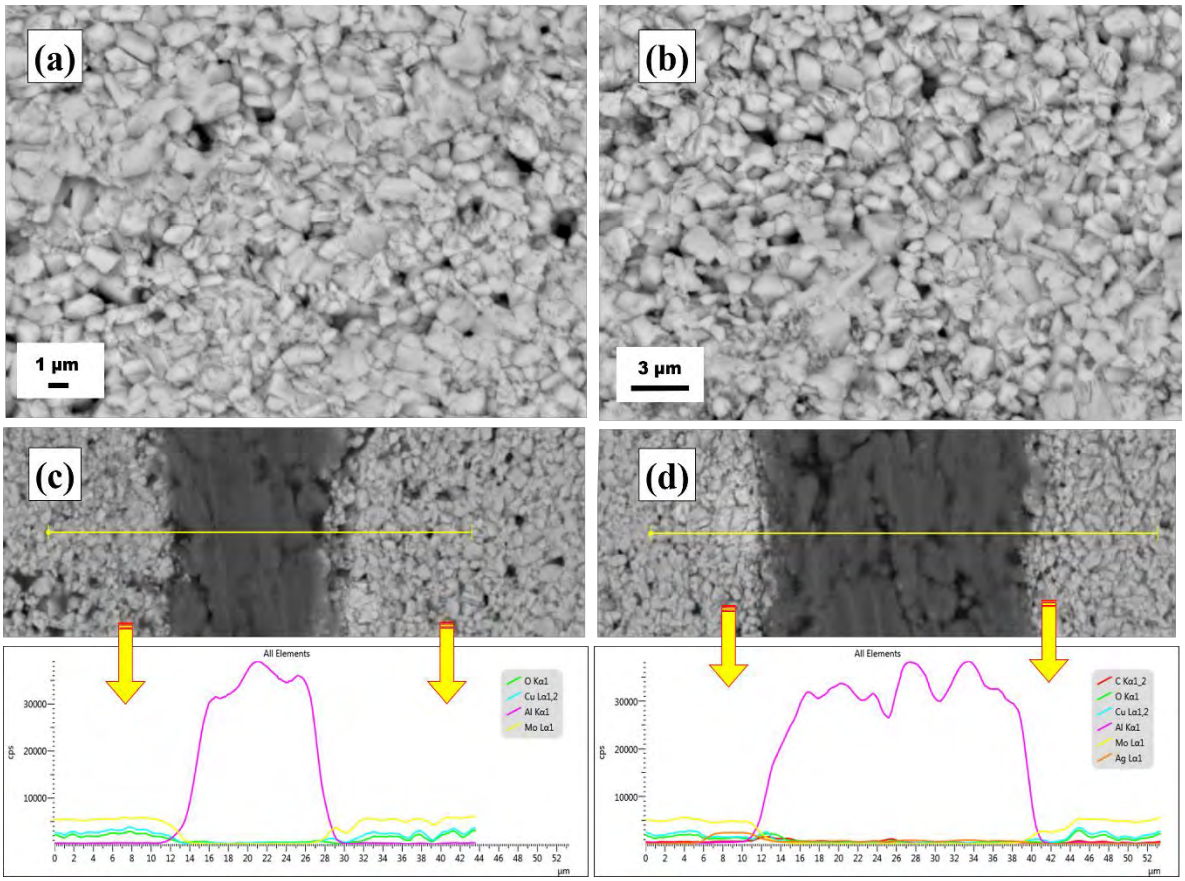

***Figure 8**: Backscattered electron (BSE) images of sintered (a) CMO and (b) CMOA substrates, cofired, (c) CMO and (d) CMOA substrates with energy dispersive X-ray analysis (EDS line mapping) of the ceramic-metal interface*

A more detailed microstructure of the green and sintered substrates were obtained from the SEM image shown in the supporting information figure S4 and figure 8 respectively. The microstructure of the green CMO and CMOA substrates with different magnifications shown in figure S4 indicated that the green tape appeared to be dense with little porosity as the polymer binder bonds the particles together during thermo-lamination. The morphology of the thermo-laminated stack revealed that the thermo-lamination conditions resulted in the merging of individual layers into a homogenous coherent body during sintering. This may correspond to the good slurry composition. The microstructure of the sintered and cofired substrates with Al ink is presented in figure 8. The sintered tape microstructure appeared to be dense and homogeneous with the removal of all organic additives. Substantial grain growth was observed and was tightly packedwith good densification, which is clear from the backscattered secondary electron images as shown in figure 8 (a & b). EDs line map shown in figure 8 (c & d) further confirmed that both substrates were free from all organics. The cofired CMO sintered substrate consisted solely of Cu, Mo and O_2 while the presence of a small amount of Ag was observed in the cofired CMOA substrate, as expected.

Aluminium powder does not react with the CMO ceramic as well as with CMOA on sintering at 650

and 500 °C respectively as reported in our earlier studies.[16,17] As evident from the BSE images and energy-dispersive X-ray analysis (EDS line mapping) of the ceramic-metal interface shown in figure 8 (c & d), no reaction layer as well as no diffusion of the electrode into the ceramicwas observed. These results indicate the chemical compatibility between the electrode and the ceramic in the multilayer ceramic substrate.

Microwave dielectric properties of substrates

The dielectric properties of the substrate play a vital role in governing the signal transmission, i.e. in determining the circuit speed because it acts as a support material for active and passive devices, and for the interconnecting conductors that make up the substantial subsystems. The dielectric properties measured at GHz frequencies are of great interest due to the active development of mobile communications.[39,40] The supporting information Table S2 represents the microwave dielectric properties of green (single layer and 5-layer vacuum laminate) while those of 5-layer vacuum laminated and sintered substrates of CMO and CMOA are given in Table 4. Both the green substrates exhibited low dielectric constant and high dielectric loss, which relates to the presence of organic additives.

Table 4: *Microwave dielectric properties of the sintered substrates*

Materials	**Microwave dielectric properties**					
	2.4 GHz		**5.1 GHz**		**9.9 GHz**	
	ε_r ±2%	**tanδ** ± (7-10%)	ε_r ±1%	**tanδ** ± (7-10%)	ε_r ±1%	**tanδ** ± (7-10%)
CMO	7.7	7.3×10^{-5}	7.6	1.8×10^{-4}	7.5	2.4×10^{-4}
CMOA	7.8	3.5×10^{-4}	7.7	3.7×10^{-4}	7.7	4.2×10^{-4}

The sintered substrates showed good microwave dielectric properties with ε_r in the range of approximately 8. For both substrates, the ε_r was almost stable over the measured frequency ranges with a slightly decreasing tendency. The developed substrates exhibited a very low loss in the range of 10^{-5} to 10^{-4} over the measured frequency ranges. However, the CMOA showed a slightly higher relative permittivity and dielectric loss compared to the CMO owing to the presence of a small amount of secondary phase. All these observations are well in line with the results achieved for the bulk samples.[16,17] These dielectric properties indicate the potential of the developed substrate materials for microwave substrate applications at high frequencies. Figure 9 represents the variation of ε_r and tanδ of the sintered CMO and CMOA substrates over the measured temperature range of -40 to 80 °C at 9.9 GHz. The relative permittivity increased with the temperature as expected.[41] For both materials, ε_r increased almost linearly from 7.4 to 7.6 (CMO) and from 7.6 to 7.7 (CMOA) without any abnormality with τ_ε values of 159 and 149 ppm/°C, respectively. The thermal stability of these

substrates could be further improved in the future by adding suitable additives. The tanδ showed some variation with increasing temperature. However, both substrates exhibited a low dielectric loss in the range of 10^{-4} over the entire measured temperature range. The dielectric properties of these substrates were compared with a commercial LTCC DuPont 9k7 sintered at 850 °C and measured by the same SPDR measuring technique, which exhibited $\varepsilon_{r,}$=7.4, tanδ = 11×10^{-4} and τ_ε =159 ppm/°C (-40 to 80 °C) at 9.9 GHz. The substrates developed in the present work had comparable ε_r and τ_ε with lower values of dielectric loss and sintering temperature than the commercial substrates. This highlights the potential of these ULTCC substrates for future microelectronic substrate applications as an environmentally friendly replacement for LTCC.

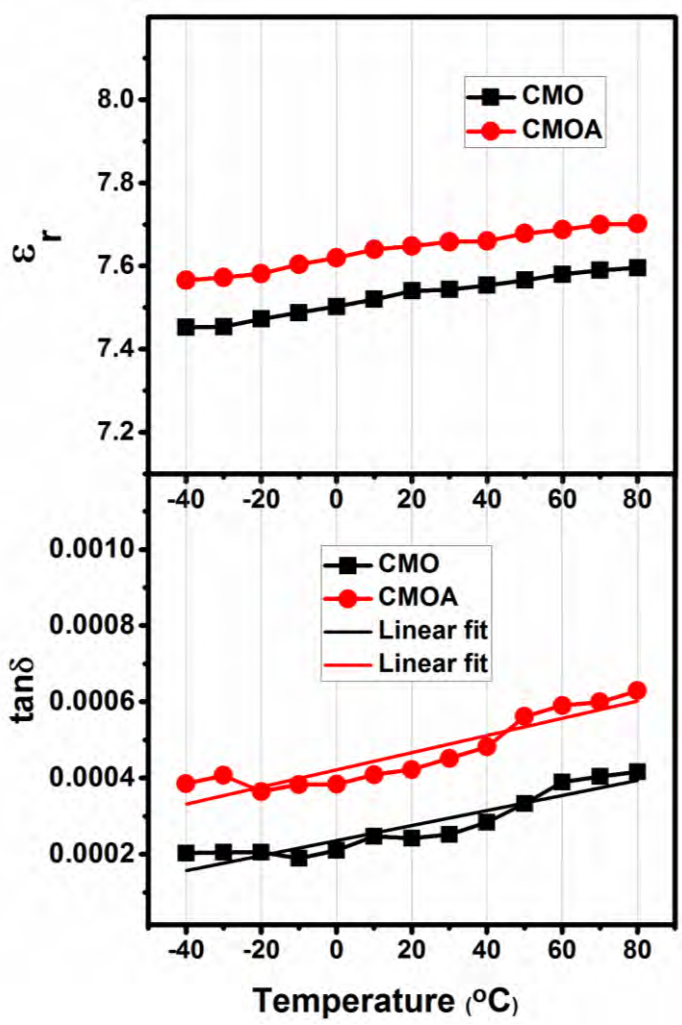

***Figure 9**: Temperature dependence of the dielectric properties of the sintered CMO and CMOA substrates.*

The coefficient of thermal expansion of substrates

The sintered CMO and CMOA substrates exhibited an average low CTE value of 4.1 and 4.6 ppm/°C respectively in the temperature range of 25-300 °C being close to the CTE value of Si (4 ppm /°C),

which enables the integration of these substrates with the semiconductor devices used in the electronics industry. This supports the prospect of these selected materials (CMO and CMOA) for device level applications.[42,43]

To highlight the importance of the present work, a comparison in the properties of some commercial substrates (LTCC) and reported HTCC, LTCC and ULTCC substrates is given in Table 5. It is clear from the table that the ULTCC substrates can achieve properties comparable to those of HTCC and LTCC substrates while having a very low sintering temperature. Moreover, a significant reduction in the sintering temperature of ULTCC systems in comparison with HTCC and LTCC fabrication temperatures further points to a future low cost and sustainable fabrication technology. The considerable reduction in the fabrication temperature reduces the CO_2emission to some extent.[51,52] Also, it should be noted that only very few ULTCCs have been used to realize substrates by tape casting as described in this work. The table emphasizes the significance of the present work in the growth of future substrate applications in the high frequency ranges.

Table5*: Comparison of the properties of some of the commercial, reported HTCC, LTCC and ULTCC substrates with those of our present work.*

Commercial and research reports on microwave substrates	**S.T** [a]**(°C)**	**Ra (nm)**	**Microwave properties**			**CTE (ppm/° C)**
			ε_r	**tanδ $\times 10^{-4}$**	**Frequency**	
Al_2O_3 [44]	1700	-	9.5-9.9	1-4	10 GHz	6-8
AlN[44]	1900	-	8.0-9.2	10	1 MHz	4.2-5.8
$ZrSiO_4$[44]	1600	-	9.2	3	5 GHz	-2.5
ZAT[@29]	1150	85	9.6	8.4	5 GHz	6.59
Sr_2ZnTeO_6(SZT)-5 wt.% of ZBPT[¤38]	900	154	12	20	5 GHz	-
$Bi4(SiO_4)_3$[36]	900	320	13.3	7	15 GHz	7.09
$LiMgPO_4$[27]	900	250	6.4	2	5 GHz	10.5
Indialite/cordierite glass-10 wt.% Bi_2O_3 [45]	900	-	6.1	1	1 MHz	3.5
$SrCuSi_4O_{10}$+5 wt.% LMZBS[*] [46]	900	560	4.8 4.7	16 19	5 GHz 15 GHz	-
$Li_2ZnTi_3O_8$(LZT)- 1 wt.% LMZBS[*47]	875	151	21.9 21.5 21.3	2 4 7	5 GHz 10 GHz 15 GHz	11.97
$Sr_2ZnSi_2O_7$+15 wt.% LMZBS[*48]	875	-	6.9	15	20 GHz	-
Dupont 9K7[Present work]	850	-	7.4	11	9.9 GHz	-
Ferro A6[44]	850	-	5.9	20	3 GHz	7

40 Al_2O_3–60 BBSZ"[49]	850	299	10.9	90	5 GHz	6.9
40 Al_2O_3–60 LABS[&50]	775	293	4.7	50	5 GHz	5.1
$LiWO_4$ [10]	650	182	5.4	0.92	5 GHz	16
Silicon dioxide-filled zinc borate glass[9]	650	-	6.4	10	1 MHz	-
$Zn_2Te_3O_8$ -titanium dioxide[11]	650	-	17.3	60	7 GHZ	-
CMO[Present work]	650	257	7.67 7.60 7.54	0.73 1.8 2.42	2.4 GHz 5.1 GHz 9.9 GHz	4.1
CMOA[Present work]	500	302	7.80 7.71 7.68	3.50 3.70 4.22	2.4 GHz 5.1 GHz 9.9 GHz	4.7

[a]S.T- Sintering temperature, [@]ZAT -0.83$ZnAl_2O_4$-0.17TiO_2 (in moles), ¤ZBPT -10 mol% ZnO – 2 mol% B_2O_3– 8 mol% P_2O_5– 80 mol% TeO_2,[*]LMZBS-20Li_2O:20MgO:20ZnO:20B_2O_3:20SiO_2,"BBSZ-35Bi_2O_3:32ZnO:27B_2O_3:6SiO_2),[&]LABS-40Li_2CO_3:10Al_2O_3:30B_2O_3:20SiO_2.

Conclusion

The ULTCC CMO and CMOA ceramic substrates were prepared by tape casting using environmentally friendly slurry compositions, followed by sintering at 650 and 500 °C respectively. The results showed that the developed slurry composition was feasible for these ULTCCs with completed burnout below 300 °C leaving very low residual carbon (less than 5%). This was at the same level as measured for the commercial LTCCs. The densification of both ceramics (≥ 95%) was close to that measured for the bulk samples, as were the dielectric properties (ε_r = 8, tanδ = 10^{-5} to10^{-4} at 2-10 GHz). Moreover, the substrates had a low CTE of around 4-5 ppm/°C, close to that of Si semiconductor, and could be cofired with embedded Al electrodes. Hence, the results show that the developed substrates fabricated by an environmentally friendly approach fulfil the demands of low residual carbon and also enable the fabrication of multilayer substrates with good mechanical, thermal and dielectric properties.

Acknowledgement

The authors are thankful to European Research Council (ERC) Project No: 24001893 and ERC POC No is 812837 for the financial support. The second author is grateful to the Ulla Tuominen Foundation project grant in 2018. This work was also partially supported by the Academy of Finland 6Genesis Flagship (Grant 318927).

Supporting Information. Sintering profile optimization of CMO substrate; high resolution C1s spectrum of green and sintered substrates (9k7, 951, CMO & CMOA); 3D AFM images of green and sintered CMO and CMOA substrates; microstructure of green laminated CMO and CMOA substrates of at different magnifications; binding energy of Cu 2p, Mo 3d, Ag 3d and O 1s in eV; microwave dielectric properties of the green tapes.

References

1. Sebastian, M. T.; Wang, H.; Jantunen, H. Low Temperature Co-fired Ceramics with Ultralow Sintering Temperature: A Review. *Curr. Opin. Solid State Mater. Sci.***2016**, 20, 151-170.
2. Roosen, A. Ceramic Substrates: Trends in Materials and Applications. *Ceram. Trans.***2000**, 106, 479-492.
3. Stiegelschmitt, A.; Roosen, A.; Ziegler, C.; Martius, S.; Schmidt, L.-P. Dielectric Data of Ceramic Substrates at High Frequencies. *J. Eur. Ceram. Soc.***2004**, 24, 1463-1466.
4. Zhang, G.; Guo, J.; Wang, H. Ultra Low Temperature Sintering Microwave Dielectric Ceramics Based Ag_2O-MoO_3 Binary System. *J. Am. Ceram. Soc.***2017**, 100, 2604-2611.
5. Varghese, J.; Siponkoski, T.; Nelo, M.; Sebastian, M. T., Jantunen, H. Microwave Dielectric Properties of Low-Temperature Sinterable α-MoO_3. *J. Eur. Ceram. Soc.***2018**, 38, 1541-1547
6. Varghese, J.; Siponkoski, T.; Teirikangas, M.; Sebastian, M. T.; Uusimäki, A.; Jantunen, H. Structural, Dielectric, and Thermal Properties of Pb Free Molybdate Based Ultralow Temperature Glass. *ACS Sustainable Chem. Eng.***2016**, 4, 3897-3904.
7. Varghese, J.; Gopinath, S.; Sebastian, M.T. Effect of Glass Fillers in $Cu_2ZnNb_2O_8$ Ceramics for Advanced Microwave Applications. *Mater. Chem. Phys.***2013**, 137, 811–815.
8. Neelakantan, U. A.; Kalathil, S. E.; Ratheesh, R. Structure and Microwave Dielectric Properties of Ulta low Temperature Cofirable BaV_2O_6 Ceramics. *Eur. J. Inorg. Chem.***2015**, 2015, 305–310.
9. Yu, H.; Ju, K.; Liu, J.; Li, Y. Tape Casting and Dielectric Properties of SiO_2-Filled Glass Composite Ceramic with an Ultra-Low Sintering Temperature. *J. Mater. Sci. Mater. Electron.***2014**, 25, 5114-5118.
10. Sasidharanpillai, A.; Kim, C. H.; Lee, C. H.; Sebastian, M. T.; Kim, H. T. Environmental Friendly Approach for the Development of Ultra-Low Firing Li_2WO_4 Ceramic Tapes. *ACS Sustainable Chem. Eng.***2018**, 6, 6849-6855.
11. Honkamo, J.; Jantunen, H.; Subodh, G.; Sebastian, M. T.; Mohanan, P. Tape Casting and Dielectric Properties of $Zn_2Te_3O_8$-Based Ceramics with an Ultra-Low Sintering Temperature. *Int. J. Appl. Ceram. Technol.***2009**, 6, 531-536.
12. Varghese, J.; Siponkoski, T.; Sobocinski, M.; Vahera, T.; Jantunen, H. Multilayer Functional Tapes Cofired at 450 ºC: Beyond HTCC and LTCC technologies. *ACS Appl. Mater. Interfaces* .**2018**, 10, 11048-11055.
13. Chen, M. Y.; Vahera, T.; His, C. S.; Sobocinski, M.; Teirikangas, M.; Peräntie, J.; Juuti, J.;

Jantunen, H. Tape Casting System for ULTCCs to Fabricate Multilayer and Multimaterial 3D Electronic Packages with Embedded Electrodes. *J. Am. Ceram. Soc.***2017**, 100, 1257-1260.

14. Pyo, S. H.; Park, J. H.; Chang, T. S.; Hatti-Kaul, R. Dimethyl Carbonate as a Green Chemical. *Curr. Opin. Green Sustain. Chem.***2017**, 5, 61-66.
15. Fiorani, G.; Perosa, A.; Selva, M. Dimethyl Carbonate: A Versatile Reagent for a Sustainable Valorization of Renewables. *Green Chem.***2018**, 20, 288-322.
16. Joseph, N.; Varghese, J.; Siponkoski, T.; Teirikangas, M., Sebastian, M.T.; Jantunen, H.; Glass Free $CuMoO_4$ Ceramic with Excellent Dielectric Properties for Ultra-Low Temperature Cofired Ceramic Applications. *ACS Sustain. Chem. Eng.* **2016**, 4, 5632-5639.
17. Joseph, N.; Varghese, J.; Teirikangas, M.; Sebastian, M.T; Jantunen, H. Ultra-Low Sintering Temperature Ceramic Composites of $CuMoO_4$ Through Ag_2O Addition for Microwave Applications. *Composites Part B.* **2018**, 141, 214-220.
18. Miguel, A. M. M.; Maider, Z.; Elizabeth, C. M.; Aitor, E. B.; Teo´filo, R.; Montse, C. C. Composition and Evolution of the Solid-Electrolyte Interphase in $Na_2Ti_3O_7$ Electrodes for Na-ion Batteries: XPS and Auger Parameter Analysis. *ACS Appl. Mater. Interfaces.***2015**, 7, 7801-7808.
19. http://srdata.nist.gov/xps/main_search_menu.aspx (2018).
20. Janezic, M. D.; Krupka, J. Split-post and split-cylinder resonator techniques: A Comparison of Complex Permittivity Measurement of Dielectric Substrates. *J. Microelectron. Electron. Packag.***2009**, 6, 97-100.
21. Krupka, J.; Gregory, A. P.; Rochard, O. C.; Clarke, R. N.; Riddle, B.; Baker-Jarvis, J. Uncertainty of Complex Permittivity Measurements by Split-Post Dielectric Resonator Technique. *J. Eur. Ceram. Soc.***2001**, 21, 2673-2676
22. Imanaka, Y. Multilayered Low Temperature Cofired Ceramics Technology, Springer, USA, **2005**.
23. Li, S.; Zhang, Q.; Yang, H.; Zou, D. Fabrication and Characterization of $Li_{1+x-y}Nb_{1-x-3y}Ti_{x+4y}O_3$ Substrates Using Aqueous Tape Casting Process. *Ceram. Int.***2009**, 35, 421-426.
24. Ferraro, P.; Hanggodo, S.; Burn, I.; Baker, A.; Qu, W. Use of Polyalkylene Carbonate Binders for Improved Performance in Multilayer Ceramic Capacitors. *Int. Symp. Microelectron.* **2011**, 2011, 000785-000788.
25. Kramer, D. P.; Santangelo, J. G.; Weber, J. J. CO_2 Copolymer Binder for Forming Ceramic Bodies and a Shaping Process Using the Same. U.S. Patent 4, 882, 110, A, November 21,

1987.

26. Kramer, D. P.; Santangelo, J. G.; Weber, J. J. CO_2 Copolymer Ceramic-Binder Composition. U.S. Patent 4,814,370A, January 15, **1988**.
27. Thomas, D.; Abhilash, P.; Sebastian, M. T. Casting and Characterization of $LiMgPO_4$ Glass free LTCC Tape for Microwave Applications. *J. Eur. Ceram. Soc.***2013**, 33, 87-93.
28. Abhilash, P.; Surendran, K. P. Glass Free, Non-Aqueous LTCC Tapes of $Bi_4(SiO_4)_3$ with High Solid Loading. *J. Eur. Ceram. Soc.***2015**, 35, 2313-2320.
29. Roshni, S. B.; Sebastian, M. T.; Surendran, K. P. Can Zinc Aluminate-Titania Composite be an Alternative for Alumina as Microelectronic Substrate? *Scientific Reports.***2017**, 7, 40839 (1-13).
30. Kingery, W. D.; Bowen, H. K.; Uhlman, D.R. Introduction to Ceramics (2nd Ed.). John Wiley and Sons, New York, **1976**.
31. Rosidah, A. Sintering of Ceramics - New Emerging Techniques. ISBN:978-953-51-0017-1, InTech, Croatia, **2012**.
32. Sebastian, M. T.; Ubic, R.; Jantunen, H. Microwave Materials and Applications. Wiley, **2017**.
33. Beisinger, M. C.; Lau, L. W. M.; Gerson, A. R.; Smart, R. S. C. Resolving Surface Chemical States in XPS Analysis of first Row Transition Metals Oxides and Hydroxides:Sc, Ti, V, Cu and Zn. *Appl. Surf. Sci.***2010**, 257, 887-898.
34. Chigrin, P. G.; Lebukhova, N. V.; Ustinov, A. Y. Structural Transformation of $CuMoO_4$ in the Catalytic Oxidation of Carbon. *Kinet. Catal.***2013**, 54, 79-84.
35. Raoufi, D.; Kiasatpour, A.; Fallah, H.R.; Rozatian, A.S.H. Surface Characterization and Microstructure of ITO Thin Films at Different Annealing Temperatures. *Appl. Surf. Sci.***2007**, 253, 9085-9090.
36. Abhilash, P.; Sebastian, M. T.; Surendran, K. P. Glass Free, Non-Aqueous LTCC Tapes of $Bi_4(SiO_4)_3$ With High Solid Loading. *J. Eur. Ceram. Soc.***2015**, 35, 2313-2320.
37. Kumar, B. R.; Rao, T. S. AFM Studies on Surface Morphology, Topography and Texture of Nanostructured Zinc Aluminum Oxide Thin Films. *Dig. J. Nanomater. Biostruct.* **2012**, 7, 1881-1889.
38. Abhilash, P.; Roshni, S. B.; Mohanan, P.; Surendran, K.P. A Facile Development of Homemade Substrate Using 'Quench Free' Glass-Ceramic Composite and Printing Microstrip Patch Antenna on it. *Mater. Des.***2018**, 137, 38-46.
39. McN Alford, N.; Penn, S. J. Sintered Alumina with Low Dielectric Loss. *J. Appl. Phys.* **1996**, 80, 5895-5898.
40. Rosidah, A. Structural and Dielectric Properties of Glass –Ceramic Substrate with Varied

Sintering Temperatures, Sintering Applications Burcu, E. Intech Open, Croatia, **2013**. DOI: 10.5772/54037.

41. Sebastian, M. T. Dielectrics for Wireless Communications, Elsevier, UK, **2008**.
42. Varghese, J.; Présumey, M.; Sebastian, M. T; Surendran, K. P. Structural, Dielectric and Thermal Properties of $Ca_9R_2W_4O_{24}$ [R–Nd, Sm] Ceramics. *Mater. Chem. Phys.* **2014**, 148, 96-102.
43. Varghese, J.; Joseph, T., Surendran, K. P.; Rajan, T. P. D.; Sebastian, M. T. Hafnium Silicate: A New Microwave Dielectric Ceramic with Low Thermal Expansivity. *Dalton Transactions*. **2015**, 44, 5146-5152.
44. Varghese, J.; Joseph, T.; Sebastian, M.T. $ZrSiO_4$ Ceramics for Microwave Integrated Circuit Applications. *Mater. Lett.***2011**, 657, 1092-1094.
45. Varghese, J.; Vahera, T.; Ohsato, H.; Iwata, M.; Jantunen H. Novel Low-Temperature Sintering Ceramic Substrate Based on Indialite/Cordierite Glass Ceramics. *Jpn. J. Appl. Phys.***2017**, 56,10PE01(1-4).
46. Manu, K.; Sebastian, M. T. Tape Casting of Low Permittivity Wesselsite–Glass Composite for LTCC Based Microwave Applications. *Ceram. Int.* **2016**, 42, 1210-1216.
47. Arun, S.; Sebastian, M.T.; Surendran, K.P. $Li_2ZnTi_3O_8$ based high κ LTCC Tapes for Improved Thermal Management in Hybrid Circuit Applications. *Ceram. Int.***2017**, 43, 5509-5516.
48. Joseph, T.; Sebastian, M.T.; Jantunen H.; Jacob M., Sreemoolanadhan, H. Tape Casting and Dielectric Properties of $Sr_2ZnSi_2O_7$-Based Ceramic–Glass Composite for Low-Temperature Co-fired Ceramics Applications. *Int. J. Appl. Ceram. Technol.* **2011**, 8,854-864.
49. Induja, I. J.; Abhilash, P.; Arun, S.; Surendran, K.P.; Sebastian, M. T. LTCC Tapes Based on Al_2O_3-BBSZ Glass with Improved Thermal Conductivity. *Ceram. Int.***2015**, 41, 13572-13581.
50. Induja, I. J.; Varma, M. R.; Sebastian, M. T. Preparation, Characterization and Properties of Alumina-Lithium Aluminium Borosilicate Glass Based LTCC Tapes. *J Mater Sci: Mater Electron.***2017**, 28, 14655-14663.
51. Sohrabi, B. H.; Lanagan, M.; Randall, C. A. Contrasting Energy Efficiency in Various Ceramic Sintering Processes. *J. Eur. Ceram. Soc.***2018**, 38, 1018-1029.
52. Varghese, J.; Ramachandran, P.; Sobocinski, M.; Vahera, T.; Jantunen H. ULTCC Glass Composites Based on Rutile and Anatase with Cofiring at 400 °C for High Frequency Applications. *ACS Sustain. Chem. Eng.***2019**, 7, 4274-4283.

Graphical Abstract